frontiers | Frontiers in Marine Science

TYPE Original Research
PUBLISHED 19 January 2023
DOI 10.3389/fmars.2023.1097177

OPEN ACCESS

EDITED BY
Sha Lou,
Tongji University, China

REVIEWED BY
Zhong Peng,
East China Normal University, China
Zhenchang Zhu,
Guangdong University of Technology, China

*CORRESPONDENCE
Peng Yao
p.yao@hhu.edu.cn
Peixiong Chen
chenpeixiong@126.com

SPECIALTY SECTION
This article was submitted to Coastal Ocean Processes, a section of the journal Frontiers in Marine Science

RECEIVED 13 November 2022
ACCEPTED 04 January 2023
PUBLISHED 19 January 2023

CITATION
Zhang R, Chen Y, Chen P, Zhou X, Wu B, Chen K, Sun Z and Yao P (2023) Impacts of tidal flat reclamation on suspended sediment dynamics in the tidal-dominated Wenzhou Coast, China.
Front. Mar. Sci. 10:1097177.
doi: 10.3389/fmars.2023.1097177

Impacts of tidal flat reclamation on suspended sediment dynamics in the tidal-dominated Wenzhou Coast, China

Rong Zhang[1,2], Yongping Chen[1,2], Peixiong Chen[3,4,5]*, Xin Zhou[2,4,5], Biying Wu[2], Kehao Chen[3], Zhilin Sun[3] and Peng Yao[1,2,6]*

[1]State Key Laboratory of Hydrology-Water Resources and Hydraulic Engineering, Hohai University, Nanjing, China, [2]College of Harbour, Coastal and Offshore Engineering, Hohai University, Nanjing, China, [3]Ocean College, Zhejiang University, Zhoushan, China, [4]The Second Institute of Oceanography, Ministry of Natural Resources, Hangzhou, China, [5]Key Laboratory of Ocean Space Resource Management Technology, Ministry of Natural Resources, Hangzhou, China, [6]State Key Laboratory of Coastal and Offshore Engineering, Dalian University of Technology, Dalian, China

Reclamation of tidal flats is one of the engineering measures of expanding land area and developing the economy in coastal areas; however, this process disturbs the natural processes of the tidal flat system. Taking the flood-tidal dominant Oufei tidal flat at the Wenzhou coast as a study area, the influences of tidal flat reclamation on tidal and suspended sediment dynamics were comprehensively investigated *via* numerical modeling. Before the reclamation, the Eulerian residual current flows alongshore and the residual sediment transport on-shore in the tidal flat area. The reclamation reduces the tidal flat area, shifting the M4 co-phase line toward the coast and squeezing the flood-dominated area. Consequently, the tidal current is weakened and the suspended sediment concentration (SSC) is reduced, but the residual sediment transport change insignificantly. The residual sediment transport in the Feiyunjiang Estuary is controlled by the tidal pumping effect. The upper estuary shows a net sediment transport landward, while a seaward transport is observed in the lower estuary, which further splits into two circulation outside the estuary. The south Oufei dike construction interferes the northern sediment circulation, resulting in the alteration of local SSC and enhancing landward sediment transport inside the estuary. The methodology and understandings arising from this study could be a good reference for the analysis of suspended sediment transport under tidal flat reclamation effects at other sites.

KEYWORDS

tidal flat reclamation, suspended sediment transport, suspended sediment concentration, tidal asymmetry, tidal waves

1 Introduction

The coastal zone is a transitional land-sea interaction area influenced by oceanic and terrestrial forcing. Since more than one-third of the world's population lives in coastal zones, it is also highly interfered with human activities (Temmerman et al., 2013; Zhu et al., 2020). Tidal flats are a crucial geomorphic unit of the coastal zone and are mainly composed of muddy deposits. Tidal flats can provide a habitat for flora and fauna to protect biodiversity, protect the coasts from storms, and increase the coastal protection capacity (Murray et al., 2019; Zhou et al., 2022). With the progress of society and the development of the economy, the reclamation of upper tidal flats has become the primary engineering method of solving the problem of land scarcity in many coastal cities worldwide, promoting economic development (Sengupta et al., 2018; Chu et al., 2022). In addition, tidal flat reclamation can effectively elevate the low-lying coastal areas which are frequently threatened by sea level rise, flooding, storm surges and other disasters (Goemans and Visser, 1987; Hoeksema, 2007; Chen et al., 2019; Pan et al., 2022). With global climate change and the intensification of human activities, tidal flats are under unprecedented pressure.

The tidal flats mainly serve as sedimentary sinks of fine-grained sediments and are high-frequency areas of land reclamation projects (Pedersen and Bartholdy, 2006; van Maren et al., 2016; Wu et al., 2018). However, tidal flat reclamation can cause a sharp reduction or even loss of sediment sinks. Consequently, the suspended sediment concentration (SSC) may increase in the surrounding channels, bringing siltation. Thus, sediment sinks shift from shallow tidal flats to nearby deep channels due to tidal flat reclamation (van Maren et al., 2016; Gao et al., 2018; Cheng et al., 2020). Meanwhile, in the tidal flat just near the sea dike, the sedimentation rate may be reduced or even turn to erosion due to strengthened tidal current velocity and wave conditions (Zhang and Chen, 2015; Cox et al., 2022). As a result, the tidal flats shift from suspended sediment sink to a source. Due to the differences in engineering designs and dynamic coastal environments, the coastal geomorphological responses to reclamation projects vary in different regions. The variations are related not only to the coastal morphology, geomorphological patterns, and hydrodynamic forces after reclamation, but also to the strength and persistence of the reclamation (Su et al., 2020; Xu et al., 2021).

Regarding tidal flats inside the estuaries, Winterwerp and Wang (2013) and Winterwerp et al. (2013) found that the reclamation of tidal flats and the deepening of navigation channels can change the properties of the original estuaries. Due to the narrowing and deepening of the tidal-dominated estuaries, the original low-turbidity estuaries have been transformed into high-turbidity. The high turbidity estuaries will further reduce the bottom friction, amplifying the upstream tidal waves, and forming an irreversible cycle. van Maren et al. (2016) reported that reclamation projects squeeze the sediment deposition area in the estuary, leading to increased SSC inside the estuary. Under increased tidal waves due to the narrowing and deepening of the estuary, the seaward sediment transport reverses landward, resulting in upstream sedimentation. Xie et al. (2017) found that similar reverse sediment transportation and sedimentation occurred in the upper estuaries in the Qiantang Estuary. They suggested continuous reclamation of the estuarine area was essential in changing sediment transport regimes. For such tidal-dominated estuaries, it is known that reclamation and channel dredging have irreversible effects on estuary evolution (van Maren et al., 2015; Wang et al., 2015). The main mechanisms can be summarized as follows: the superiority of the flood tide is strengthened, the amplitude of the tidal waves is enhanced, the trend of the net sediment transport is changed, and the natural properties of the estuary are affected.

The Oufei tidal flat on the Wenzhou coast in China is located between the Feiyunjiang River estuary and the Oujiang River estuary (Chen et al., 2021) (Figure 1). It is a typical muddy tidal flat with a slow deposition trend, featured by a flood-dominant tide. In the last ten years, due to economic development, a series of reclamation projects have been progressively carried out in the Oufei tidal flat, advancing the shoreline to the sea (Mei et al., 2019; Cai et al., 2021). Different from the reclamation inside the estuary, which may cause the regime shift of the estuary properties, it is unclear on the effects of reclamation on accreting open tidal flats and on the adjacent estuaries.

In this study, we take the Oufei tidal flat as a research site, aiming to explore the impacts of reclamation on suspended sediment dynamics in the tidal-dominated tidal flat and the adjacent estuary. To this end, a numerical model was established to simulate the tidal and sediment dynamics before and after the reclamation. By analysis of the tidal current pattern, SSC distribution, and the residual suspended sediment transport in the study area, the influence mechanism of the reclamation project on the sediment dynamics was identified. Section 2 introduces the study area and the numerical model; Section 3 illustrates the results on tidal and sediment dynamics before and after the reclamation; Section 4 discusses the corresponding mechanisms by analyzing tidal asymmetry and decomposing on net sediment transport; the conclusions are listed in Section 5.

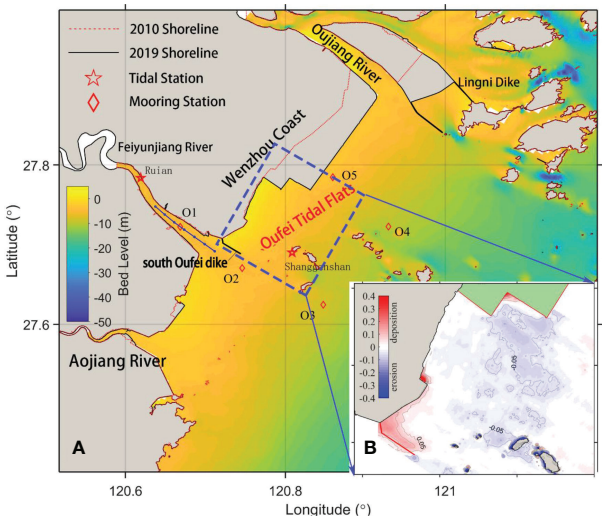

FIGURE 1
(A) Bathymetric map of the Oufei tidal flat area in 2019 and **(B)** morphological changes of Oufei tidal flat between 2010 and 2019 (unit: m/yr). The blue line in **(A)** inside the Feyunjiang River defines six locations (points) used to conduct sediment flux decomposition in Section 4.

2 Materials and methods

2.1 Study area

The Oufei tidal flat is located in the eastern part of the Wenzhou coast. It is characterized by a straight shoreline and an accreting tidal flat (Figure 1). The tides around the Oufei tidal flat region are regular semi-diurnal tides, and the M2 tidal components are dominant (Xu, 2020; Chen et al., 2021). The average tidal range is 4.4 m and can be classified as a macro-tidal area. Influenced by the shape of the local topography, the tidal current in the Oufei tidal flat is mainly reciprocating, with the flood current pointing toward the northwest and the ebb current directing toward the southeast. According to long-term measurements at Nanji Island Oceanographic Station, the waves are mainly wind-waves, with an annual average wave height $H_{1/10}$ of about 1 m.

The Oujiang River and the Feiyunjiang River flow into the sea to the north and the south of the Oufei tidal flat, respectively. The annual average discharge of the Oujiang River is 470 m^3/s, and that of the Feiyunjiang River is 75 m^3/s (Li, 2010). A large amount of sediment from the Yangtze Estuary is transported to the offshore area of the Oufei tidal flat by longshore currents. Subsequently, the local tidal currents and waves push this sediment toward the tidal flats (Chen et al., 2021). The SSC in the Feiyunjiang River Estuary is much higher than in the Oufei tidal flat area, leading to the maximum turbidity zone being located in the estuary.

2.2 Model setup

Based on the open-source Delft3D software, a numerical model that considers both the tidal current and sediment transport in the Oufei tidal flat was constructed. The flow module of the Delft3D software is mainly based on shallow water equations and the Boussinesq assumption for an incompressible fluid. Since the Wenzhou Coast is a macro-tidal-dominated and well-mixed coast, and the Feiyunjiang Estuary is classified as well-mixed at most times of the year according to Simmons's classification method (Jin and Sun, 1992), we apply a depth-averaged (i.e., 2D) way to compute tidal current and sediment transport. More details can be found in the user manual of Delft3D (Deltares, 2011). The suspended sediment transport was calculated using the two-dimensional advection-diffusion equation:

$$\frac{\partial(HS)}{\partial t}+\frac{1}{G_\xi}\frac{\partial(HUS)}{\partial \xi}+\frac{1}{G_\eta}\frac{\partial(HVS)}{\partial \eta} = \frac{1}{G_\xi}\frac{\partial}{\partial \xi}\left(v_s\frac{H}{G_\xi}\frac{\partial S}{\partial \xi}\right)+\frac{1}{G_\eta}\frac{\partial}{\partial \eta}\left(v_s\frac{H}{G_\eta}\frac{\partial S}{\partial \eta}\right)-F_s, \quad (1)$$

where S is the average depth of the SSC (kg/m^3); t is time (s); ξ and η are orthogonal curvilinear coordinates under the Cartesian coordinate system (m); G_ξ and G_η are the Lame coefficients in the coordinate system; U and V are the average velocity components along the water depth (m/s) in directions ξ and η, respectively; ζ is the tidal elevation (m); d is the water depth (m); H = ζ + d is the total water depth (m); v_s is the turbulent diffusion coefficient for suspended sediment (m^2/s); F_s is the sediment exchange item between the sediment bed and water; $F_s = D_b - E_b$; D_b is the sediment deposition flux on the seabed surface; and E_b is the scour flux on the seabed.

The Oufei tidal flat and its adjacent estuaries are dominated by fine sediments. The median grain size of the suspended sediment is around 6 μm (Wu et al., 2015). Therefore, the Partheniades–Krone equation was used to calculate the sediment exchange term between the sediment bed and water. The sedimentation flux (D_b) is:

$$D_b=\begin{cases}\omega_s S_b\left(1-\frac{\tau_{bs}}{\tau_d}\right) & \tau_{bs}\le\tau_d\\ 0 & \tau_{bs}>\tau_d\end{cases}, \quad (2)$$

where ω_s is the sedimentation velocity of the cohesive sediment (m/s); S_b is the sediment concentration (kg/m^3); τ_{bs} is the effective shear stress (N/m^2); and τ_d is the critical deposition shear stress (N/m^2). The erosion flux (E_b) is written as follows:

$$E_b=\begin{cases}M\left(\frac{\tau_{bs}}{\tau_e}-1\right) & \tau_{bs}\ge\tau_e\\ 0 & \tau_{bs}<\tau_e,\end{cases} \quad (3)$$

where τ_e is the critical erosion shear stress (N/m^2); and M is the erosion coefficient related to the sediment properties, which reflects the erosion resistance of the sediment in the seabed.

The domain of the Oufei Model (OM) ranges from 119°E to 124° E and from 32°N to 36.5°N. The entire area was about 200 km×550 km. The total number of grids was 104133. The grid resolution ranges from 30m in the Feiyunjiang River Estuary to 100 in the nearshore area of the Oufei tidal flat. The tidal elevation data were used as the open boundary conditions, provided by the two-dimensional tidal current model of the East China Sea (Su et al., 2015). The shallow water area (i.e., tidal flats) was processed into the moving boundary using the wet-dry boundary condition. According to the grain size analysis of the surface sediments in the Oufei tidal flat conducted by Wu et al. (2015), the bed sediment of the model was set as silt, with a particle size of 8 μm (slightly larger than the suspended sediment size, i.e., 6 μm), a dry density of 500 kg/m^3, a critical starting shear stress of 0.5 Pa, and a settling velocity (flocculation settling velocity) of 2.4 mm/s.

Two cases were set up based on the OM. One uses the shorelines and bathymetric data in 2010 (namely, 2010 model) representing the condition before reclamation. The other uses shorelines and bathymetric data in 2019 (namely, 2019model) to represent the condition after reclamation. The bathymetric data in 2010 and 2019 in the Oufei tidal flat were derived from field surveys, while the nautical charts in the corresponding period were used for Feiyunjiang Estuary and the seaward area. These data were processed to the same vertical datum (i.e., China national height datum 1985). An additional case (caseSL) was setup by keeping the bathymetry the same as in 2010 and the shoreline the same as in 2019, to explore the impacts of shoreline changes.

2.3 Model verification

The calculation time of the pre-reclamation case (that is, the 2010 model) was from October 1, 2010, to November 1, 2010, and the calculation time step was 30 s, which satisfies the stability conditions of the Courant number. During the one-month simulation, the bed

level changes were also simulated. However, the resulting bed level changes were small because the simulation period only covered two spring-neap tidal cycles. Figure 1 shows the distribution of the measurement stations for tidal elevation, velocity and SSC in the Oufei tidal flat in 2010. The tidal elevation, tidal current, and SSC at each station were calculated using the model and were compared with the measured data for verification. Figures 2–4 shows part of model verification results. See Supplementary Materials for details. In Supplementary Materials, the model verification results of 2019model were also listed. The results demonstrate that the calculated values of the tide level, flow velocity, flow direction, and SSC are in good agreement with the measured values, and the errors are within 10%. The errors between simulation and measurement were mainly due to the inaccurate bathymetric data (e.g., the depth near O1 is from the nautical charts), ignorance of waves and winds, complexity in sediment transport modelling. It can be considered that the model can accurately simulate the hydrodynamic and sediment characteristics of the Oufei tidal flat in 2010 and 2019, respectively.

2.4 Data analysis

Based on the validated numerical model (i.e., the 2010 model) of the Oufei tidal flat, the tidal current and sediment transport during one month in 2010 and 2019 were calculated, respectively. The tidal elevation, flow current, SSC, and suspended sediment transport in the study area before and after reclamation were compared and analyzed.

The tidal ratio, $(H_{K_1}+H_{O_1})/H_{M_2}$, in the mouth of the Feiyunjiang River ranges from 0.18 to 0.28, and the sea area is a normal semi-diurnal tidal area. The tidal asymmetry characteristics are mainly generated by the interaction between the semi-diurnal tide (M_2) and the shallow water tide (M_4). Therefore, the harmonic analysis is mainly focused on the M_2 and M_4 sub-tides. The M_4/M_2 amplitude ratio and ($2M_2$–M_4) relative phase parameters defined by Friedrichs and Aubrey (1988) were used to analyze the asymmetry of the tides.

$$A = \frac{H_{M_4}}{H_{M_2}}, \tag{4}$$

$$G = 2\varphi_{M_2} - \varphi_{M_4}, \tag{5}$$

where H_{M_2} and H_{M_4} are the amplitudes of the M_2 and M_4 tides, respectively; and φ_{M_2} and φ_{M_4} are the phase lags of the M_2 and M_4 tides, respectively. The tidal deformation coefficient A is the amplitude ratio of the M_4 tide to the M_2 tide, and the tidal deformation coefficient G is the phase difference between the M_4 tide and M_2 tide. $A > 0.01$ indicates a large deformation during the tidal wave propagation. G represents the dominant relationship between the high and low tides in the tidal asymmetry.

To analyze the characteristics and main factors controlling the residual suspended sediment transport in the study area, the suspended sediment flux decomposition method proposed by Dyer (1997) was adopted to decompose the residual transport rate, $F(kg/(m \cdot s))$, of the suspended sediment during the entire tidal cycle T.

$$\begin{aligned} F &= \frac{1}{T}\int_0^T \int_0^1 huc dz dt \\ &= h_0 u_0 c_0 + c_0 \overline{h_t u_t} + u_0 \overline{h_t c_t} + h_0 \overline{u_t c_t} + \overline{h_t u_t c_t} + h_0 \overline{c_v}\ \ \overline{u_v} + h_0 \overline{c_{vt} u_{vt}} \\ &= T_1 + T_2 + T_3 + T_4 + T_5 + T_6 + T_7, \end{aligned} \tag{6}$$

where h, u and c are the total water depth, tidal current velocity and SSC respectively; T is tidal period; the subscript 0 means the tidal average; the subscript t tidal variation, the subscript v means the vertical variation and the subscript vt denotes the variation over tidal cycle and water depth; overbar means the average over tidal cycle; angled bracket means average over water depth. Totally, suspended

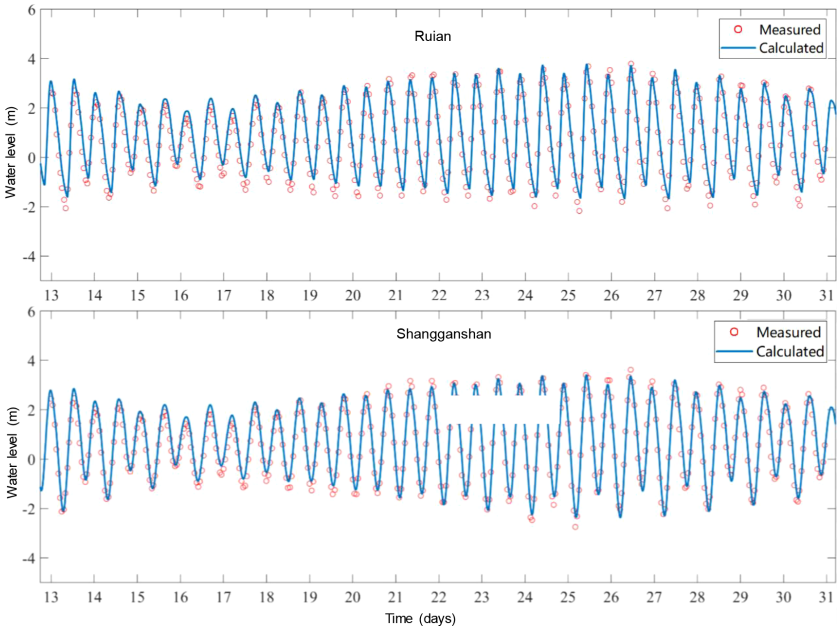

FIGURE 2
Comparison of calculated and measured water levels. The measurement period was from October 13 to October 31, 2010, at the different stations.

10.3389/fmars.2023.1097177

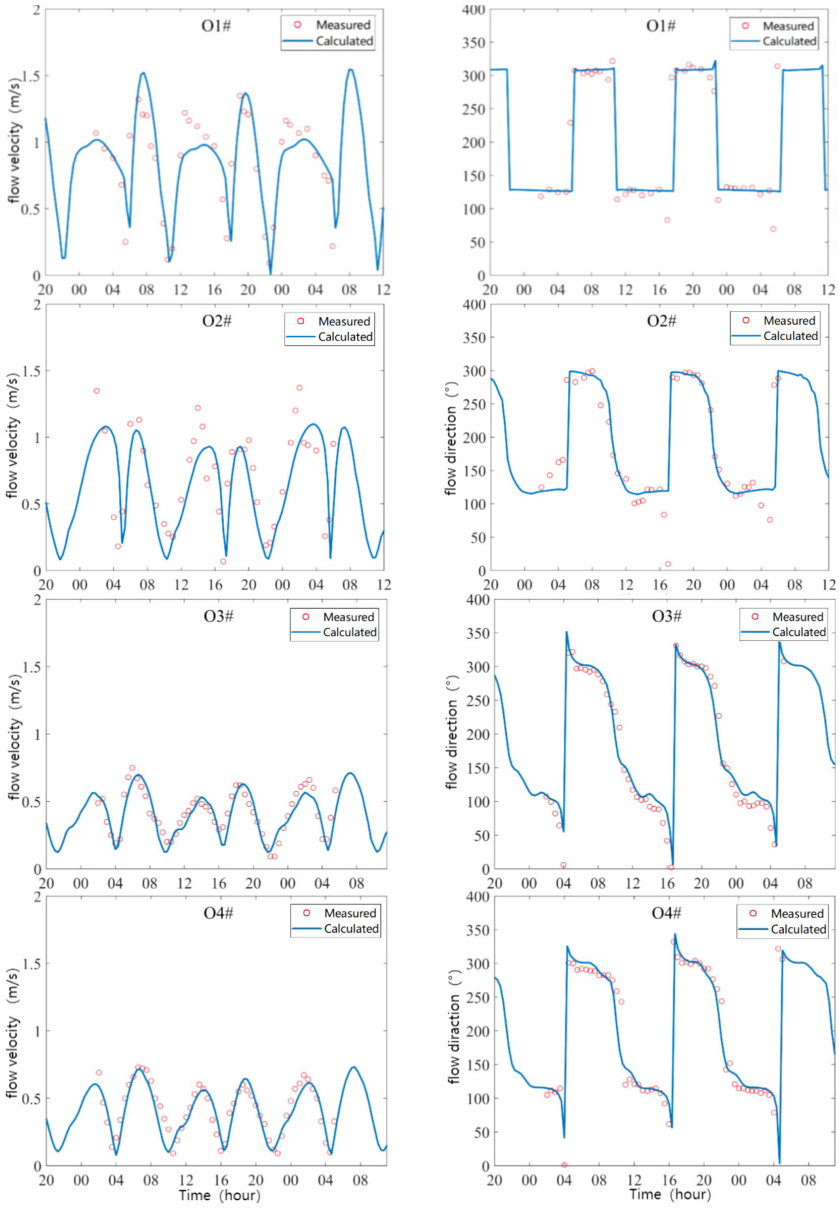

FIGURE 3
Comparison of the simulated and measured flow velocity during spring tide. The measurement period was from October 24 to 25 in 2010.

sediment flux can be decomposed into seven terms. T_1 is the suspended sediment transport term caused by the Eulerian residual current; T_2 is the Stokes drift transport term; and $T_1 + T_2$ is the Lagrange advection transport term. T_3 is caused by the phase difference between the tidal elevation and SSC. T_4 is the phase difference between the tidal current and SSC, which is mainly caused by the sediment settling and erosion lag, and it is also known as the tidal trapping effect. T_5 is the phase difference among the tidal elevation, tidal current, and SSC, which is caused by the settling lag and erosion lag. $T_3 + T_4 + T_5$ is related to the tidal pumping term; T_6 is the gravity circulation term along the vertical direction of the estuary; and T_7 is the difference between the vertical distributions of the velocity and sediment concentration caused by the tidal wave deformation. $T_6 + T_7$ is the residual vertical circulation transport term, which is related to the shear diffusion effect.

3 Results

3.1 Variations of the tidal water level

Figure 5 shows the co-tidal and co-amplitude charts of the M_2 and M_4 tides before and after the tidal flat reclamation. Before the reclamation, the M_2 tide propagated east to west, and the phase lag increased from 34° to 42°. The amplitude increased toward the shore, and the peak was about 2.40 m. The M_2 tidal amplitude in the Oufei tidal flat area increased initially and then decreased from the sea toward the land, and the peak value was about 2.40 m. After the reclamation, the M_2 tidal distribution was the same as before. Influenced by the south Oufei dike, the amplitude of the southern shelter area increased, and the peak amplitude area of 2–2.4 m contracted toward the shore.

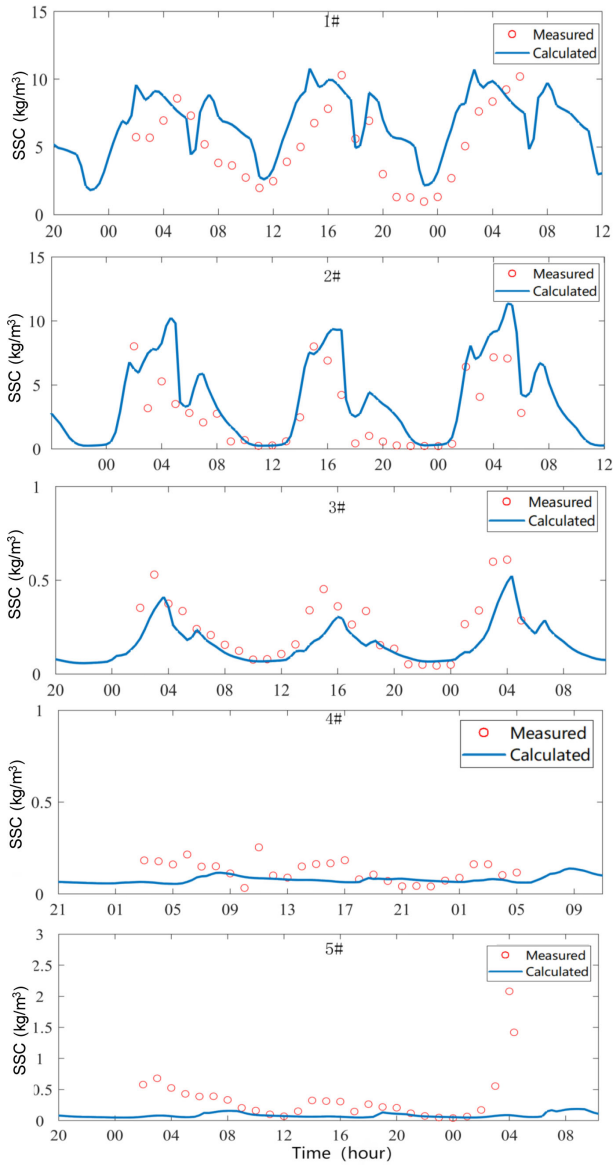

FIGURE 4
Comparison of the simulated and measured SSCs during spring tide. The measurement period was from October 24 to 25 in 2010.

Before the reclamation, the M_4 tidal amplitude gradually increased from the sea toward the land, exhibiting significant shallow water effects. The M_4 tidal amplitude was slightly smaller than the M_2 tidal amplitude, and the peak value was only 0.40 m. The M_4 co-tidal line and amplitude distribution were similar. The co-tidal line is parallel to the coastline, and the 280 -340° co-tidal lines almost coincide, indicating the effects of a sloped topography. After the reclamation, the overall pattern of the M_4 did not change significantly, but each co-tidal line was shifted toward the shore.

3.2 Variations of the tidal current

The tidal current is one of the leading forces shaping the landform of the Wenzhou Coast. Figure 6 shows the differences in the tidal current field between the flooding and ebb peak before and after the reclamation. The reclaimed area is shown in green. From the south of the reclaimed area to the Feiyunjiang Estuary, the flow direction exhibits noticeable deflection after the reclamation.

During flood peak, the tidal current flows perpendicular to the shoreline near the Oufei tidal flat before the reclamation, while the tidal currents change to flow along the artificial shoreline after the reclamation. The maximum flow velocities during flood tide decrease more than 0.4 m/s after the reclamation. The construction of the south Oufei dike blocks part of the water exchange between the tidal flat and the estuary, decreasing flow velocity (~0.4 m/s) near the dike. The dike also prolongs the estuary, enlarging the flow velocity (0.1-0.2 m/s) at the prolonged estuary section, while the flow velocity decreased inside the estuary (0.1 m/s). Furthermore, the flow velocity around the offshore islands varies significantly, up to 0.4 m/s.

During ebb peak, the changes in both flow direction and flow magnitude caused by reclamation, are relatively small compared to flood tide. For example, the ebb flow velocity only reduces as large as 0.4 m/s near the reclaimed dike, while the reduction in the offshore area is not significant. During ebb tide, the south Oufei dike near estuary reduces velocity 0.05-0.1 m/s, which provides sheltering effect on the nearby tidal flat It worth noting that there are also changes in the flow directions and magnitudes near the offshore islands, but these changes are all concentrated in local areas.

The residual current refers to the movement of the remaining water body after the current separates from the cyclical tidal current movement, which is related to the long-term transport direction of the sediment along the coast. The monthly averaged Eulerian residual current distribution in the Oufei tidal flat area before and after reclamation was calculated (Figure 7). Before the reclamation, the tidal flow in the tidal flats area was predominantly in the along-shore direction toward the Feiyunjiang Estuary. There was a strong tongue-shaped residual current spreading from the estuary towards sea. The velocity of the residual current was between 0.04 and 0.12 m/s. Around the offshore islands, there were several clockwise circulations and localized high-velocity areas. The average velocity was 0.07 m/s.

After the reclamation, the residual flow velocity in the southern corner of the reclamation area increased significantly (by 0.12 m/s). There is a circumfluence zone on both sides of the south Oufei dike, and the velocity decreases slightly, while the residual velocity increases locally at the head of the dike and its northern sheltered area, with a maximum increase of 0.06 m/s. In general, due to the reclamation, the distribution of the residual current in the southern corner of the reclamation area and near the south Oufei dike changed greatly, while the impact on the rest of the sea area was not significant.

CaseSL shows the reclamation impacts on velocity magnitude if only changing the shorelines (Figure 8). The obvious velocity variations occur near the reclamation dikes and the changes in velocity magnitude is more significant during ebb (i.e., as large as 0.4 m/s). In the offshore islands area, the velocity variations before and after reclamation are within 0.05 m/s during flood tide, and within 0.1 m/s during ebb. This indicates that the impacts of tidal flat reclamation on velocity is limited around these islands. However, the changes in velocities around the reclamation area and these islands after reclamation may influence the local bathymetric changes. The changes of bathymetry in turn influences the local flow velocity. Hence, the cumulative impact due to the shoreline change still needs further study.

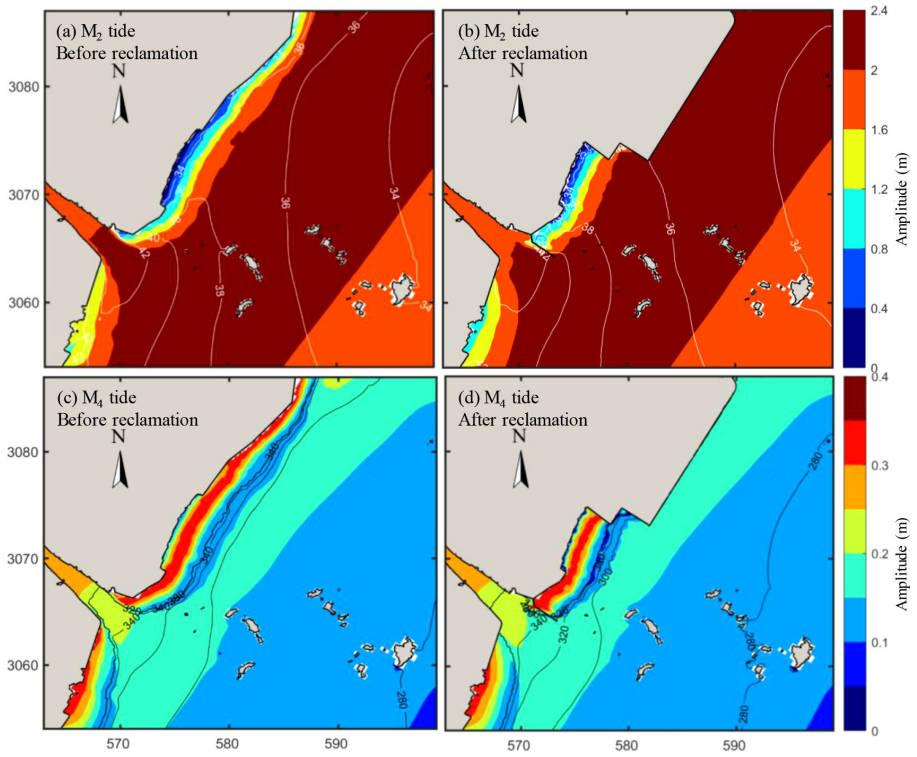

FIGURE 5
Co-tidal and co-amplitude charts before and after reclamation: M2 tidal constituent (a) before reclamation and (b) after reclamation; M4 tidal constituent (c) before reclamation and (d) after reclamation.

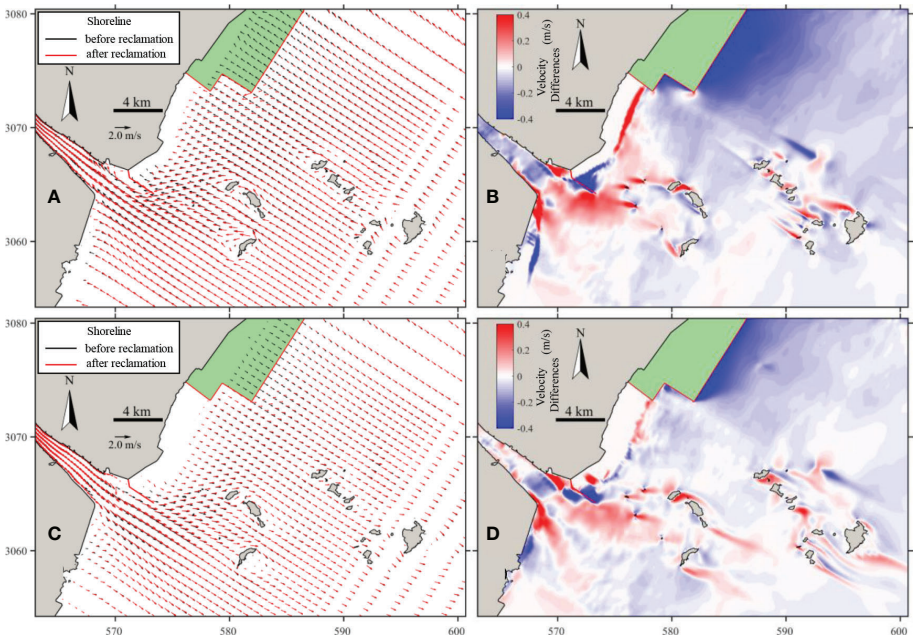

FIGURE 6
Tidal current field during spring tide before and after reclamation. Flow vectors comparisons during **(A)** flood peak and **(C)** ebb peak; Differences in velocity magnitude during **(B)** flood peak and **(D)** ebb peak. The reclamation area is shown in green area and the south Oufei dike is shown in red line near the estuary.

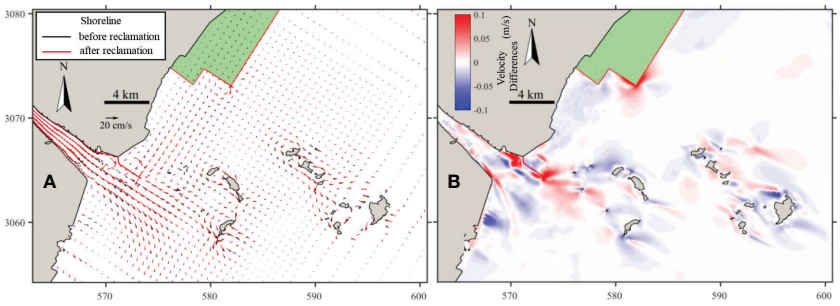

FIGURE 7
Residual tidal current for two spring-neap cycles before and after reclamation. **(A)** Flow vector comparison; **(B)** differences in velocity magnitude.

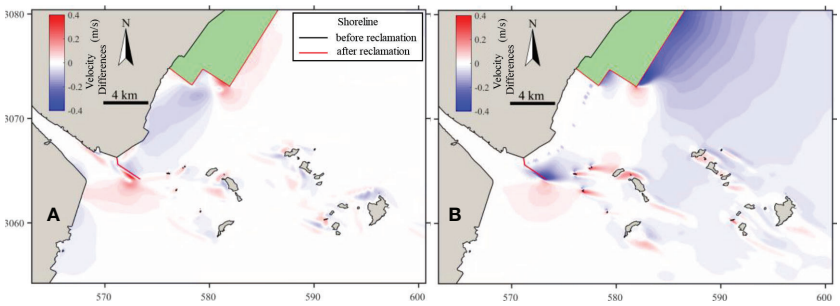

FIGURE 8
Differences in velocity magnitude during **(A)** flood peak and **(B)** ebb peak of spring tide of only changing shorelines (caseSL-2010model). Note that, caseSL keeps the bathymetry as the same, and only the shoreline changes.

3.3 Variations of suspended sediment dynamics

Figures 9A, B show the average SSC distribution over the spring tide before and after the reclamation. The SSC shows a similar distribution pattern before and after the reclamation, i.e., the SSC is high inside the estuary (larger than 14 kg/m^3) and gradually decreases in the seaward direction. Meanwhile, the SSC in the Oufei tidal flat is rather smaller. In the Feiyunjiang Estuary, the average SSC during spring tide decreased after the reclamation, with a maximum reduction value of 4 kg/m^3 (Figure 9C). The SSC in the northern reclaimed area also exhibited an overall decreasing trend, with an average decrease of about 1 kg/m^3. The SSC increases only in the sheltered area of the south Oufei dike and around the offshore islands.

Figure 9D shows the differences in the average SSC in the full spring-neap tidal cycle before and after the reclamation. The overall change in SSC is similar to that of the spring tide, but with a smaller magnitude. That is, the SSC slightly increases by about 0.2 kg/m^3 in the northeast area of the estuary and slightly decreases by about 0.5 kg/m^3 on the southwest side and on both sides of the south Oufei dike.

Figure 10 shows the changes of residual suspended sediment transport in the study area before and after the reclamation. It can be seen from Figure 10A that the suspended sediment was transported toward the tidal flat before the reclamation, resulting in the accreting tidal flat there. Inside the Feiyunjiang Estuary, the sediment transports landward in the upper estuary, whereas it directs seaward in the lower estuary. After the suspended sediment was exported from the estuary, the suspended sediment was divided into two parts, which formed a clockwise circulation to the south and a counterclockwise circulation to the north. The residual sediment was eventually transported to the estuary and the nearshore area.

After the reclamation, the residual sediment transport depicts an along-shore direction instead of on-shore. But the changes in magnitude is too small to be shown in Figure 10B. Inside the estuary the landward and seaward transport still exists, but the separation point moves seaward. This is because the construction of the south Oufei dike extends the estuary, increasing the distance of sediment entering the sea. Thus, the residual sediment transport in the upper estuary is increased, while it is decreased in the lower estuary. Outside the estuary, there are alternating increases and decreases from north to south, with changes in transport magnitude not exceeding 5×10^{-4} m^3/s/m.

In summary, the impact of the northern tidal flat reclamation on the sediment transport is relatively limited, while the construction of the south Oufei dike near the estuary mouth has a significant impact on the direction and strength of the residual sediment transport in and near the estuary.

4 Discussions

4.1 Effects of the tidal flat reclamation on the tidal asymmetry

The Oufei tidal flat is in a slow accreting state and featured by the flood-dominant tide. Since the tide, especially the tidal asymmetry,

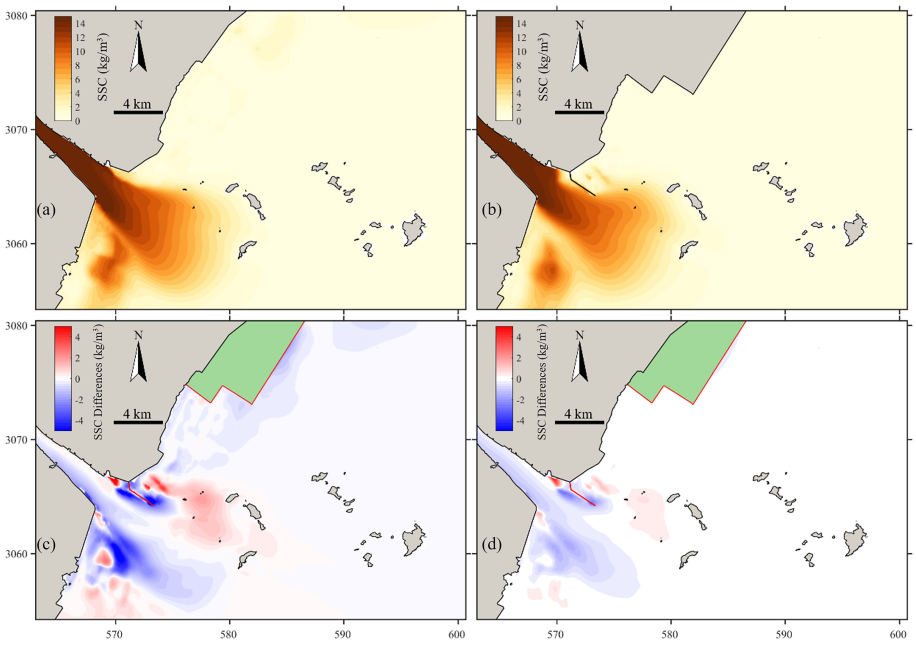

FIGURE 9
Tidal-averaged SSC during the spring tide **(A)** before and **(B)** after the reclamation; and the differences in the tidal-averaged SSC during **(C)** the spring tide and **(D)** a full spring-neap tide cycle before and after the reclamation.

plays a primary role in the morphodynamics of the Oufei tidal flat, it is necessary to investigate the effects of the reclamation influences on the tidal asymmetry.

Figure 11 shows the spatial distribution characteristics of the tidal asymmetry coefficient amplitude ratio (A) and tidal deformation coefficient (G) before and after the reclamation of the Oufei tidal flat. The tidal amplitude ratios A in the nearshore area exceeded the limit of 0.01, indicating that the tidal waves experienced significant deformation under the influences of the topography when they reached the shallow area of the Oufei tidal flat. The amplitude ratio at the mouth of the Feiyunjiang River (0.1–0.2) was smaller than that in the nearshore area of the Oufei tidal flat (0.3–0.6). This indicates that the M_4 tide was more enhanced than the M_2 tide in the nearshore area. After the reclamation, the amplitude ratios in the offshore and nearshore area did not change much. Only the amplitude ratio in the circumfluence zone on the north side of the south Oufei dike increased slightly, while the amplitude ratio in the shelter area on the south side decreased.

Before and after the reclamation, the tidal phase differences in the study area were all between 0° and 180°, confirming that the tidal current during flood tide was larger than the ebb current, and the flood tide duration was shorter than the ebb duration, i.e., the tide asymmetry is flood-dominant. The flood-dominancy gradually increased with decreasing water depth from the sea toward the land. The tidal deformation coefficient G was close to 90°, and the tidal waves tend to exhibit the maximum positive asymmetry. After the reclamation, the contours of the tidal deformation coefficient G shifted toward the shore, indicating that the flood-dominancy was slightly weakened and the sediment transport capacity of the tidal current was weakened, which may be the reason for the decrease in the suspended sediment concentration in this area.

4.2 Effects of the tidal flat reclamation on the suspended sediment transport

To further understand the mechanisms of the suspended sediment transport in the estuary and to identify the effects of the tidal flat reclamation, the residual suspended sediment transport was decomposed into the advection term and the tidal pumping term using the flux decomposition method as mentioned in Section 3. Figure 12 depicts the spatial distribution of flux decomposition before and after the reclamation. In addition, six locations were set along the estuary section (blue line in Figure 1), and the sediment transport rate over tidal cycles and the contribution of each decomposed component at each point were extracted. The results are presented in Figure 13.

Regarding the advection term, there is overall transport toward the sea outside the estuary with a transport rate larger than 0.3 kg/(m · s). The sediment transport is parallel to the tidal flat area with a relatively small magnitude. Outside the estuary, a clockwise transport pattern exists. According to the T1 and T2 terms of each calculation point inside the estuary (Figure 13A), the Eulerian residual current transport term (T1) was toward the sea, whereas the Stokes drift term (T2) was toward the land. The T2 term is comparable to the T1, hindering the upstream transport of the suspended sediment toward the sea. As a result, the advection transport term (T1+T2) of the suspended sediment inside the estuary contributes little to the residual transport of sediment (Figure 13B). Before and after reclamation, the distribution of advection transport terms was slightly reduced except the area around the south Oufei dike (P7).

With respect to the tidal pumping term, it depicts a landward sediment transport in the Oufei tidal flat with a relatively small magnitude. Outside the estuary, there is a seaward sediment transport direction in the middle, while landward sediment transports are distinguishable in the south and north estuary, respectively. Inside

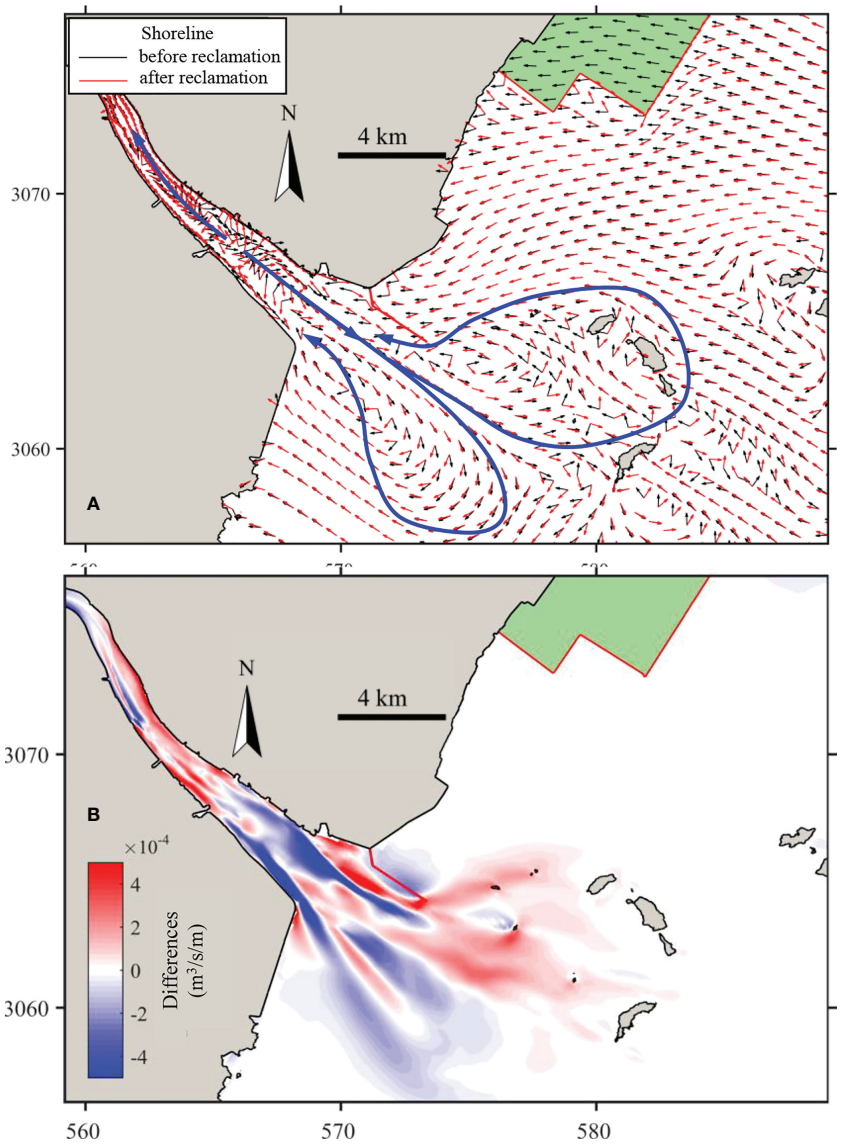

FIGURE 10
Differences in **(A)** residual sediment transport direction and **(B)** magnitude during one month before and after the reclamation.

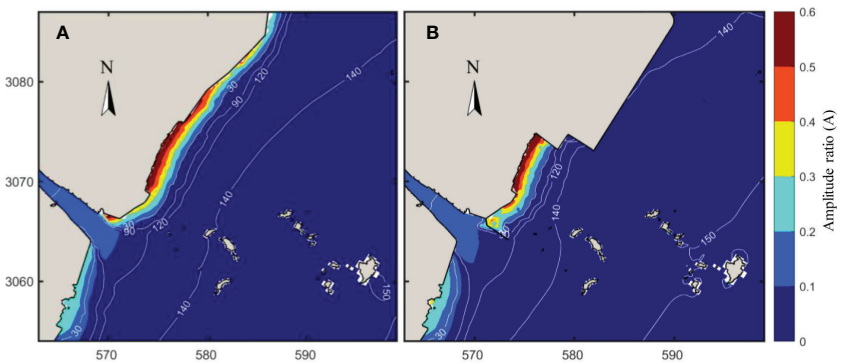

FIGURE 11
Spatial distributions of tidal asymmetry parameters **(A)** before and **(B)** after the reclamation. Note: the background map represents the amplitude ratio **(A)**, and the contour lines represent the phase difference (G).

10.3389/fmars.2023.1097177

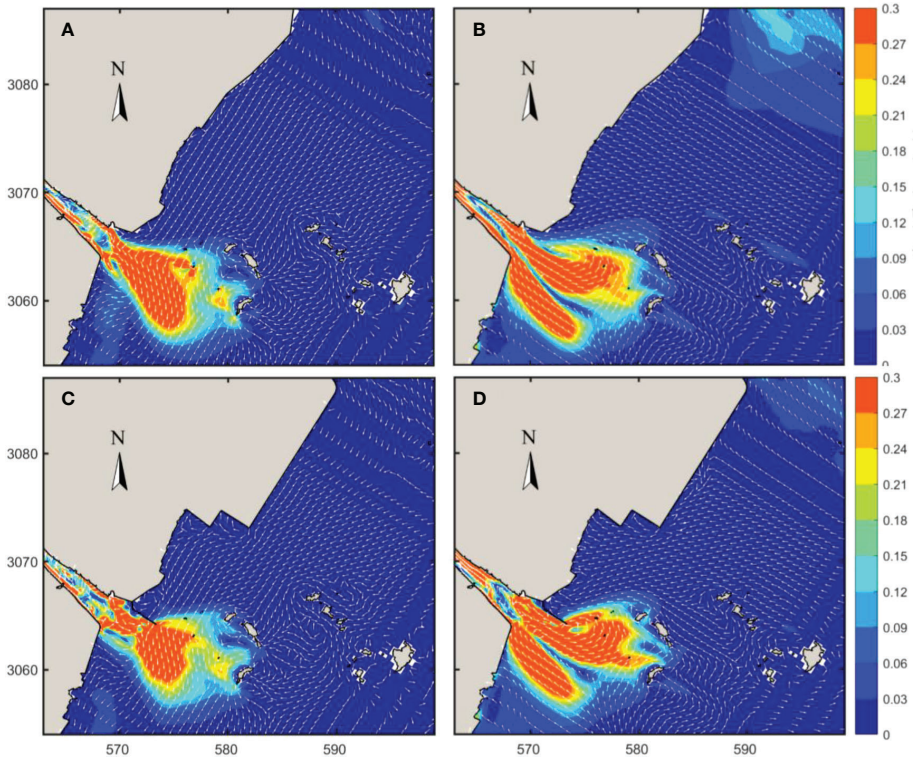

FIGURE 12
Decomposition of the residual suspended sediment transport over a spring-neap tidal cycle **(A, B)** before and **(C, D)** after the reclamation. **(A, C)** Distribution of advection transport term; and **(B, D)** tidal pumping term. The units are kg/m/s.

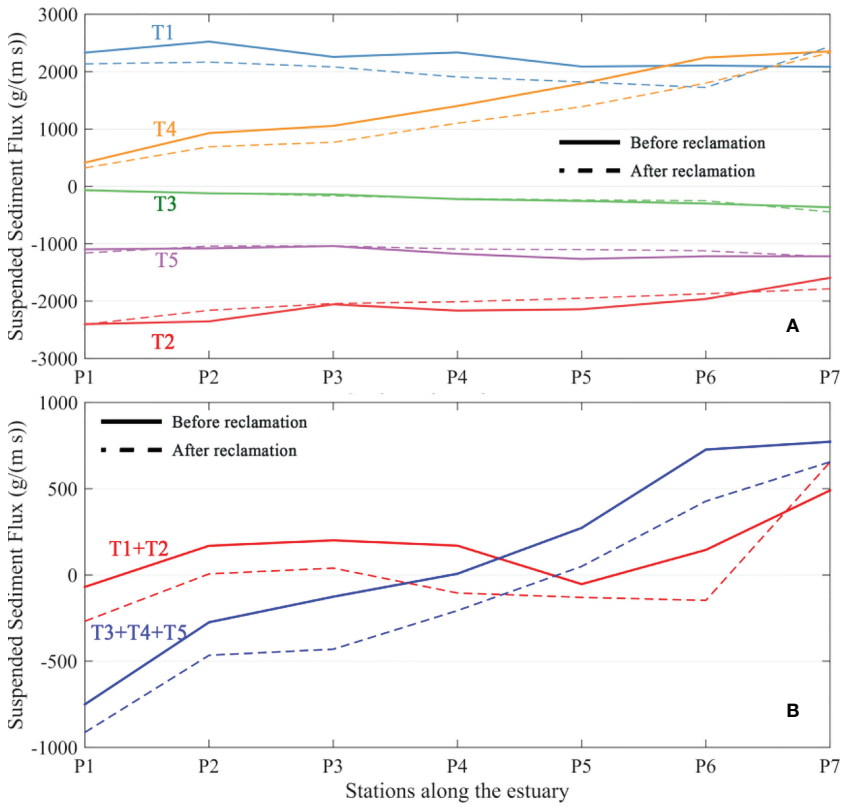

FIGURE 13
Contributions of different decomposition components to suspended sediment flux at different positions in the estuary: **(A)** five decomposition components (T1 to T5); **(B)** advection (T1+T2) and tidal pumping terms (T3+T4+T5). Note that seaward is positive, point 1 is upstream of the estuary, and other points are distributed successively downstream with an interval of 1600 m.

the estuary, the residual sediment is transported landward in the upper part, whereas it directs seaward near the mouth. The tidal pumping induced transport pattern is in line with the overall residual sediment transport shown in Figure 10A, indicating that the tidal pumping term (induced by tidal asymmetry) is the critical factor controlling the sediment transport in the Oufei tidal flat region.

The tidal pumping term inside the Feiyunjiang Estuary shows that the contributions of the T4 and T5 were more significant (Figure 13A). The T4 term points to the sea, and the intensity increases toward the sea. T4 term represents the relationship between the asymmetry of the tidal current and the suspended sediment concentration. That is, the suspended sediment transport caused by the ebb tide is more significant than that caused by the flood tide, resulting in the residual transport of the sediments toward the sea. In addition, the seaward increase in T4 indicates an enhancement of the tidal asymmetry at the mouth. T5 term shows a landward transport, and the intensity slightly increases seaward. T5 term represents the relationship between the tidal elevation asymmetry, the tidal current asymmetry, and the SSC. It reveals that the sediment transport in the mouth is greater at high tide than at low tide, resulting in residual sediment transport toward the land. T4 and T5 terms are in the same magnitude, more or less, leading to the residual sediment transport in opposite directions in the upper and lower estuary (Figure 13B). After the construction of the south Oufei dike, the length of the estuary was extended, strengthening the landward transport.

4.3 Limitations and remarks for future research

Effects of waves on residual sediment transport. There are significant seasonal variations in wave climates. In winter, the most frequent wave is from the NNE to NE direction, while in summer, it is from the E-ESE direction. Moreover, the wave height in winter is more significant than that in summer. The annual average $H_{1/10}$ wave height is about 1 m. Therefore, there would be seasonal differences in sediment transport induced by waves. While both the Oufei tidal flat and the Feiyunjiang Estuary are dominated by the tide, it is still necessary to understand the contribution of the wave on residual sediment transport and the impacts of reclamation in different temporal scales (e.g., tidal cycles, seasonal and annual).

Morphological changes and the contribution of reclamation. Comparing surveyed bathymetries makes it possible to obtain morphological changes in different periods. As shown in Figure 1B, during 2010-2019, the sedimentation mainly occurred in the upper tidal flat and the area sheltered by the south Oufei Dike, while slight erosion (annual mean erosion rate smaller than 0.05m) can be found in the lower tidal flat and seaward areas. Together with the velocity and SSC variations before and after reclamation, the sedimentation near the south Oufei Dike is due to reduced velocity and sediment transport. However, the residual sediment transport variations before and after reclamation in the lower tidal flat area were too small to be recognized. On the one hand, the morphological change was a gradual and feedback process with the tidal current, wave, and sediment transport. On the other hand, reclamation was also gradual in the past decades. The construction of each reclamation dike involves a chain reflection between hydrodynamics, sediment transport, and bed level changes. Hence, it is difficult to accurately reveal morphological change and the contribution of reclamation by comparing only the changes in residual sediment transport between two snap-shot runs. A morphodynamic model should be utilized to understand the contribution of the reclamation on morphological changes.

5 Conclusions

Through numerical modeling, the impacts of tidal flat reclamation on the suspended sediment dynamics in a flood-dominant and accreting coast have been analyzed. The main conclusions are as follows:

(1) In the Oufei tidal flat area, the M_4 tidal amplitude gradually increases from the sea toward the land, enhancing the flood-dominancy in the shallow tidal flat and promoting on-shore sediment transport. The tidal flat reclamation weakens the flood-dominancy near the reclamation area, which leads to a more pronounced tidal current velocity reduction (~0.4 m/s) during flood tide, and reduces the SSC there. But the intensity of the residual transport of the suspended sediment did not change significantly after the reclamation.

(2) In the Feiyunjiang Estuary, the SSC and the residual transport intensity of the suspended sediment in the Feiyunjiang Estuary are controlled by the tidal pumping effect, with the magnitude of ten times greater than that at the Oufei tidal flat. The residual sediment, transport landward in the upper estuary, while seaward transport is distinguishable in the lower estuary. The residual sediment transport depicts two circulation patterns outside the estuary. The south Oufei dike construction interferes the northern sediment circulation, resulting in the alteration of local SSC and enhancing landward sediment transport inside the estuary.

Data availability statement

The original contributions presented in the study are included in the article/Supplementary Material. Further inquiries can be directed to the corresponding authors.

Author contributions

RZ: Conceptualization, methodology, formal analysis, visualization, and writing—original draft. YC: Conceptualization, investigation, and writing—review and editing. PC: Conceptualization and writing—review and editing. XZ: Formal analysis, visualization, and writing—review. BW: Visualization and writing—review and editing. KC: Writing—review and editing. ZS: Writing—review and editing. PY: Conceptualization, methodology, investigation, formal analysis, writing— review and editing. All authors contributed to the article and approved the submitted version.

Funding

This study was supported by grants from the National Natural Science Foundation of China (52201320, 51979076), the Fundamental

Research Funds for the Central Universities of China (B220202078), the Postdoc International Exchange Program of China (YJ20210073), the Scientific Research Fund of the Second Institute of Oceanography, Ministry of Natural Resources, China (JG1801), and the Open Fund of the State Key Laboratory of Coastal and Offshore Engineering (LP2207).

Conflict of interest

The authors declare that the research was conducted in the absence of any commercial or financial relationships that could be construed as a potential conflict of interest.

Publisher's note

Supplementary material

The Supplementary Material for this article can be found online at: https://www.frontiersin.org/articles/10.3389/fmars.2023.1097177/full#supplementary-material

References

Cai, J. X., Pan, G. F., and Chen, P. X. (2021). Analysis of the characteristics and dynamic mechanism of scouring and silting changes in oufei tidal flat before and after the reclamation project. *J. Mar. Sci.* 39 (03), 63–71. doi: 10.3969/j.issn.1001-909X.2021.03.007

Cheng, Z., Jalon-Rójas, I., Wang, X. H., and Liu, Y. (2020). Impacts of land reclamation on sediment transport and sedimentary environment in a macro-tidal estuary. *Estuarine Coast. Shelf Sci.* 242, 106861. doi: 10.1016/j.ecss.2020.106861

Chen, Y., Li, J., Pan, S., Gan, M., Pan, Y., Xie, D., et al. (2019). Joint probability analysis of extreme wave heights and surges along china's coasts. *Ocean Eng.* 177, 97–107. doi: 10.1016/j.oceaneng.2018.12.010

Chen, P., Sun, Z., Zhou, X., Xia, Y., Li, L., He, Z., et al. (2021). Impacts of coastal reclamation on tidal and sediment dynamics in the rui'an coast of China. *Ocean Dynamics* 71, 323–341. doi: 10.1007/s10236-021-01442-3

Chu, N., Yao, P., Ou, S., Wang, H., Yang, H., and Yang, Q. (2022). Response of tidal dynamics to successive land reclamation in the lingding bay over the last century. *Coast. Eng.* 173, 104095. doi: 10.1016/j.coastaleng.2022.104095

Cox, J. R., Leuven, J. R. F. W., Pierik, H. J., van Egmond, M., and Kleinhans, M. G. (2022). Sediment deficit and morphological change of the Rhine–meuse river mouth attributed to multi-millennial anthropogenic impacts. *Continental Shelf Res.* 244, 104766. doi: 10.1016/j.csr.2022.104766

Deltares (2011). *Delft3D-FLOW user manual. 3.15 ed* (Delft, The Netherlands: Deltares (WL).

Dyer, K. R. (1997) *Estuaries: A physical introduction, 2nd edition* (Chichester: JohnWiley and Sons). Available at: http://eu.wiley.com/WileyCDA/WileyTitle/productCd-0471974714.html (Accessed June 27, 2015).

Friedrichs, C. T., and Aubrey, D. G. (1988). Non-linear tidal distortion in shallow well-mixed estuaries: A synthesis. *Estuarine Coast. Shelf Sci.* 27, 521–545. doi: 10.1016/0272-7714(88)90082-0

Gao, G. D., Wang, X. H., Bao, X. W., Song, D., Lin, X. P., and Qiao, L. L. (2018). The impacts of land reclamation on suspended-sediment dynamics in jiaozhou bay, qingdao, China. *Estuarine Coast. Shelf Sci.* 206, 61–75. doi: 10.1016/j.ecss.2017.01.012

Goemans, T., and Visser, T. (1987). The delta project: The Netherlands experience with a megaproject for flood protection. *Technol. Soc.* 9, 97–111. doi: 10.1016/0160-791X(87)90034-0

Hoeksema, R. J. (2007). Three stages in the history of land reclamation in the Netherlands. *Irrigation Drainage* 56, S113–S126. doi: 10.1002/ird.340

Jin, Y. H., and Sun, Z. L. (1992). Mixing characteristics ofsalt water and fresh water in Chinese estuaries. *Acta Geographica Sin.* 47 (2), 165–173.

Li, M. G. (2010). The effect of reclamation in areas between islands in a complex tidal estuary on the hydrodynamic sediment environment. *J. Hydrodynamics Ser. B* 22, 338–350. doi: 10.1016/S1001-6058(09)60063-9

Mei, Y. P., Cai, T. L., Wang, X. K., Xia, X. M., and Jia, J. J. (2019). Evaluation on the suitability of mud flat reclamation based on intertidal morphodynamics. *Mar. Sci. Bull.* 38 (06), 707–718. doi: 10.11840/j.issn.1001-6392.2019.06.013

Murray, N. J., Phinn, S. R., DeWitt, M., Ferrari, R., Johnston, R., Lyons, M. B., et al. (2019). The global distribution and trajectory of tidal flats. *Nature* 565, 222–225. doi: 10.1038/s41586-018-0805-8

Pan, Y., Yin, S., Chen, Y. P., Yang, Y. B., Xu, C. Y., and Xu, Z. S. (2022). An experimental study on the evolution of a submerged berm under the effects of regular waves in low-energy conditions. *Coast. Eng.* 176, 104169. doi: 10.1016/j.coastaleng.2022.104169

Pedersen, J. B. T., and Bartholdy, J. (2006). Budgets for fine-grained sediment in the Danish wadden Sea. *Mar. Geology* 235, 101–117. doi: 10.1016/j.margeo.2006.10.008

Sengupta, D., Chen, R., and Meadows, M. E. (2018). Building beyond land: An overview of coastal land reclamation in 16 global megacities. *Appl. Geogr.* 90, 229–238. doi: 10.1016/j.apgeog.2017.12.015

Su, M., Gong, Z., Yao, P., Pu, J., and Lu, Y. (2020). Investigation on factors of influence on long-term morphodynamic evolution of a multi-outlets estuarine-delta system: A case study of the lingding bay, pearl river delta. *J. Coast. Res.* 95, 664–668. doi: 10.2112/SI95-129.1

Su, M., Yao, P., Wang, Z. B., Zhang, C. K., and Stive, M. J. F. (2015). Tidal wave propagation in the yellow Sea. *Coast. Eng. J.* 57, 1550008-1-155008–29. doi: 10.1142/S0578563415500084

Temmerman, S., Meire, P., Bouma, T. J., Herman, P. M. J., Ysebaert, T., and De Vriend, H. J. (2013). Ecosystem-based coastal defence in the face of global change. *Nature* 504, 79–83. doi: 10.1038/nature12859

van Maren, D. S., Oost, A. P., Wang, Z. B., and Vos, P. C. (2016). The effect of land reclamations and sediment extraction on the suspended sediment concentration in the ems estuary. *Mar. Geol.* 376, 147–157. doi: 10.1016/j.margeo.2016.03.007

van Maren, D. S., Winterwerp, J. C., and Vroom, J. (2015). Fine sediment transport into the hyper-turbid lower ems river: the role of channel deepening and sediment-induced drag reduction. *Ocean Dyn.* 65, 589–605. doi: 10.1007/s10236-015-0821-2

Wang, Z. B., Van Maren, D. S., Ding, P. X., Yang, S. L., Van Prooijen, B. C., De Vet, P. L. M., et al. (2015). Human impacts on morphodynamic thresholds in estuarine systems. *Cont. Shelf Res.* 111, Part B, 174–183. doi: 10.1016/j.csr.2015.08.009

Winterwerp, J. C., and Wang, Z. B. (2013). Man-induced regime shifts in small estuaries–I: theory. *Ocean Dynamics* 63, 1279–1292. doi: 10.1007/s10236-013-0662-9

Winterwerp, J. C., Wang, Z. B., Braeckel, A.v., Holland, G.v., and Kösters, F. (2013). Man-induced regime shifts in small estuaries–II: A comparison of rivers. *Ocean Dynamics* 63, 1293–1306. doi: 10.1007/s10236-013-0663-8

Wu, C. S., Huang, S.c., Luo, X. X., Mu, J. B., and Zhao, X. (2015). Characteristics of surface sediment grain size in oufei tidal flat and adjacent sea area and hydrodynamic responses. *Mar. Sci. Bull.* 34 (04), 399–406. doi: 10.11840/j.issn.1001-6392.2015.04.006

Wu, Z., Milliman, J. D., Zhao, D., Cao, Z., Zhou, J., and Zhou, C. (2018). Geomorphologic changes in the lower pearl river delta 1850–2015, largely due to human activity. *Geomorphology* 314, 42–54. doi: 10.1016/j.geomorph.2018.05.001

Xie, D., Pan, C., Wu, X., Gao, S., and Wang, Z. B. (2017). Local human activities overwhelm decreased sediment supply from the changjiang river: Continued rapid accumulation in the hangzhou bay-qiantang estuary system. *Mar. Geol.* 392, 66–77. doi: 10.1016/j.margeo.2017.08.013

Xu, H. (2020). Numerical study on the impact of sanjiangkou reclamation in wenzhou on coastal hydrodynamics. *Dalian Univ. Technol.*

Xu, C., Zhou, C., Ma, K., Wang, P., and Yue, X. (2021). Response of water environment to land reclamation in jiaozhou bay, China over the last 150 years. *Front. Mar. Sci.* 8. doi: 10.3389/fmars.2021.750288

Zhang, C. K., and Chen, X. D. (2015). Offshore environmental changes and countermeasures in response to large-scale tidal flat reclamation. *J. Hohai Univ. (Natural Sciences)* 43 (5), 424–430. doi: 10.3876/j.issn.1000-1980.2015.05.006

Zhou, Z., Wu, Y., Fan, D., Wu, G., Luo, F., Yao, P., et al. (2022). Sediment sorting and bedding dynamics of tidal flat wetlands: Modeling the signature of storms. *J. Hydrology* 610, 127913. doi: 10.1016/j.jhydrol.2022.127913

Zhu, Z., Vuik, V., Visser, P. J., Soens, T., van Wesenbeeck, B., van de Koppel, J., et al. (2020). Historic storms and the hidden value of coastal wetlands for nature-based flood defence. *Nat. Sustain* 3, 853–862. doi: 10.1038/s41893-020-0556-z